

Construction of a Hollow Spherical Covalent Organic Framework with Olefin and Imine Dual Linkages Based on Orthogonal Reactions

Jingtao Hu,[†] Junjie Zhang,[‡] Zhangxiang Lin,[‡] Lili Xie,^{†,} Saihu Liao,[†] Xiong Chen^{†,*}*

[†]Key Laboratory of Molecule Synthesis and Function Discovery (Fujian Province University),
State Key Laboratory of Photocatalysis on Energy and Environment, College of Chemistry,
Fuzhou University, Fuzhou 350108, China

[‡]Key Laboratory for Analytical Science of Food Safety and Biology (Ministry of Education),
College of Chemistry, Fuzhou University, Fuzhou 350108, China

[‡]Qingyuan Innovation Laboratory, Quanzhou 362801, China

Corresponding Authors

*xielili@fzu.edu.cn (X. L.); *chenxiong987@fzu.edu.cn (X. C.)

Table of Contents:

Section S1. Materials and Instrumentation

Section S2. Synthetic Procedures

Section S3. Extensive screening of synthetic conditions

Section S4. FT-IR Spectra Analysis

Section S5. ^{13}C CP/MAS NMR Spectra Analysis

Section S6. Structural Modeling Method and Powder X-Ray Diffraction Analysis

Section S7. Scanning Electron Micrographs Analysis

Section S8. Transmission Electron Micrographs Analysis

Section S9. Thermogravimetric Analysis

Section S10. Chemical Stability Analysis

Section S11. Water contact angle on the surface of COF-FD1

Section S12. N_2 adsorption and desorption Analysis

Section S13. Pore size distribution of COF-FD1

Section S14. Fluorescence spectra

Section S15. References

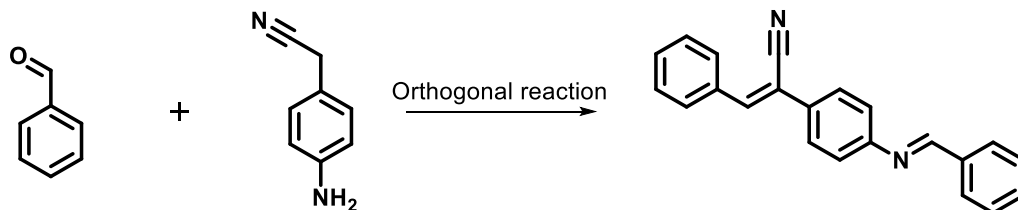
Section S1. Materials and Instrumentation

Materials. All reagents, unless otherwise noted, were purchased from commercial sources and used without further purification.

Instrumentation. ^1H NMR and ^{13}C NMR spectra were recorded on JMTC-500/54/JJ (500 MHz). FT-IR spectra were recorded with a Nicolet AVATAR360 instrument. Solid-state NMR experiments were performed on a Bruker AVANCE III 500 MHz spectrometer. Powder X-ray diffraction (PXRD) patterns were recorded on a Rigaku Ultima IV diffractometer (Japan) equipped with $\text{Cu}/\text{K}\alpha$ radiation ($\lambda = 1.5418 \text{ \AA}$) under a scan rate of 0.02 degree/min. The thermal properties of COF materials were evaluated using a thermogravimetric analysis (TGA) instrument (Labsys Evo Setline) over the temperature range of 25 to 1000 °C under nitrogen atmosphere with a heating rate of 10 °C/min. The nitrogen adsorption and desorption isotherms were measured at 77 K using a Micromeritics ASAP 2460 system. The pore-size-distribution curves were obtained from the adsorption branches using non-local density functional theory (NLDFT) method. Field emission scanning electron microscopy (FESEM) observations were performed on a FEI Nova NanoSEM 230 microscope with an accelerating voltage of 10 kV and a working distance of 1.5 mm. Transmission Electron Microscopy (TEM) images were acquired on Hitachi HT7700 operated at an accelerating voltage of 100 kV. High-resolution mass spectra (HRMS) were recorded on Thermo Fisher Scientific. UV-Vis absorption spectra were recorded on PerkinElmer Lambda750. The fluorescent spectra were recorded on Hitachi F4600. The water contact angle (CA) was measured on a JC2000C machine.

Section 2. Synthetic Procedures

Synthesis of (Z)-2-(4-[(E)-benzylidene] amino) phenyl)-3-phenylacrylonitrile (BAPP)



benzaldehyde 2-(4-aminophenyl)acetonitrile (Z)-2-(4-[(E)-benzylidene]amino)phenyl)-3-phenylacrylonitrile

A 10 mL Schlenk tube was charged with 4-aminobenzyl cyanide (0.132 g, 1 mmol), benzaldehyde (0.212 g, 2 mmol), and methanol (4 mL). Afterward, 0.4 mL of NaOH (4 M) was added to the mixture, and then the mixture was sonicated for 5 min; the resulting reaction mixture was allowed to stand at room temperature for 12 h, yielding BAPP (0.2684 g, 87%). ^1H NMR (500 MHz, chloroform-*d*): δ 8.49 (s, 1H), 7.95 – 7.89 (m, 4H), 7.72 (d, $J = 8.2$ Hz, 2H), 7.55 (s, 1H), 7.52 – 7.42 (m, 6H), 7.29 (d, $J = 8.2$ Hz, 2H). ^{13}C NMR (126 MHz, chloroform-*d*): δ 161.1, 152.9, 141.5, 136.0, 133.9, 132.1, 131.9, 130.6, 129.4, 129.1, 129.0, 127.0, 121.7, 118.1, 111.3. HRMS: m/z calcd for $\text{C}_{22}\text{H}_{16}\text{N}_2$ $[\text{M} + \text{H}]^+$, 309.1347; found, 309.1381. Mp: 117 °C.

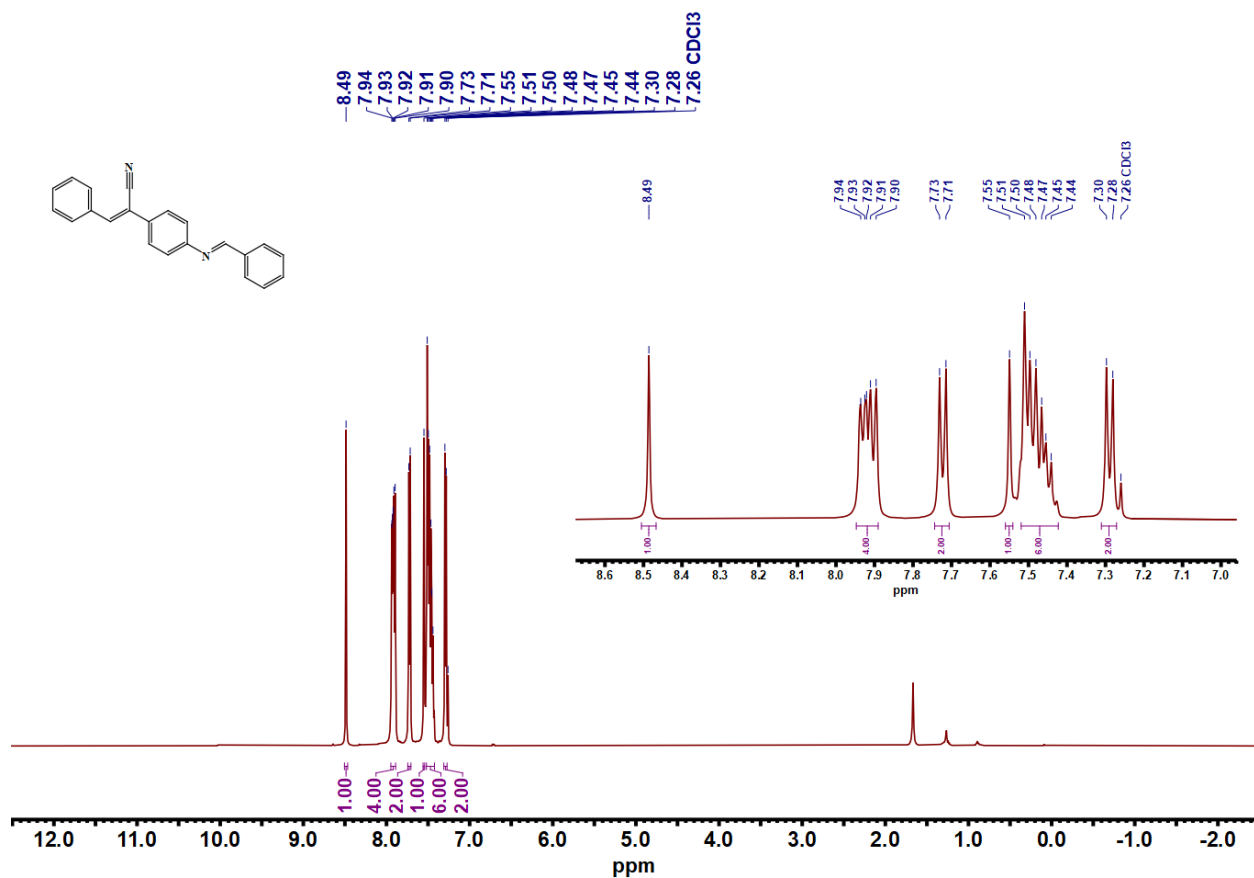


Figure S1. ¹H NMR spectrum of BAPP. Inset showing the zoom portion.

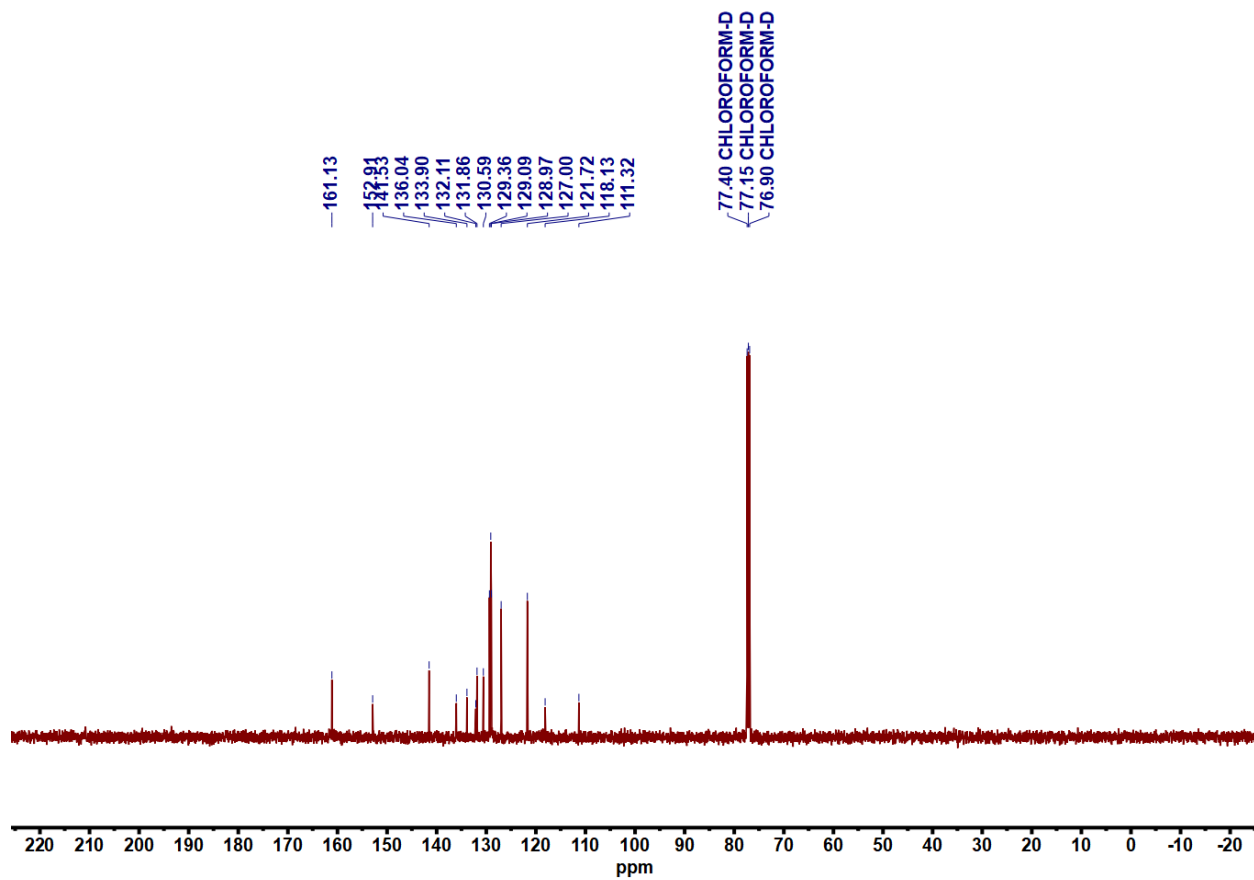


Figure S2. ¹³C NMR spectrum of BAPP.

BAPP #28 RT: 0.15 AV: 1 NL: 3.10E9 T:
FTMS + p ESI Full ms [100.0000-800.0000] 309.1381

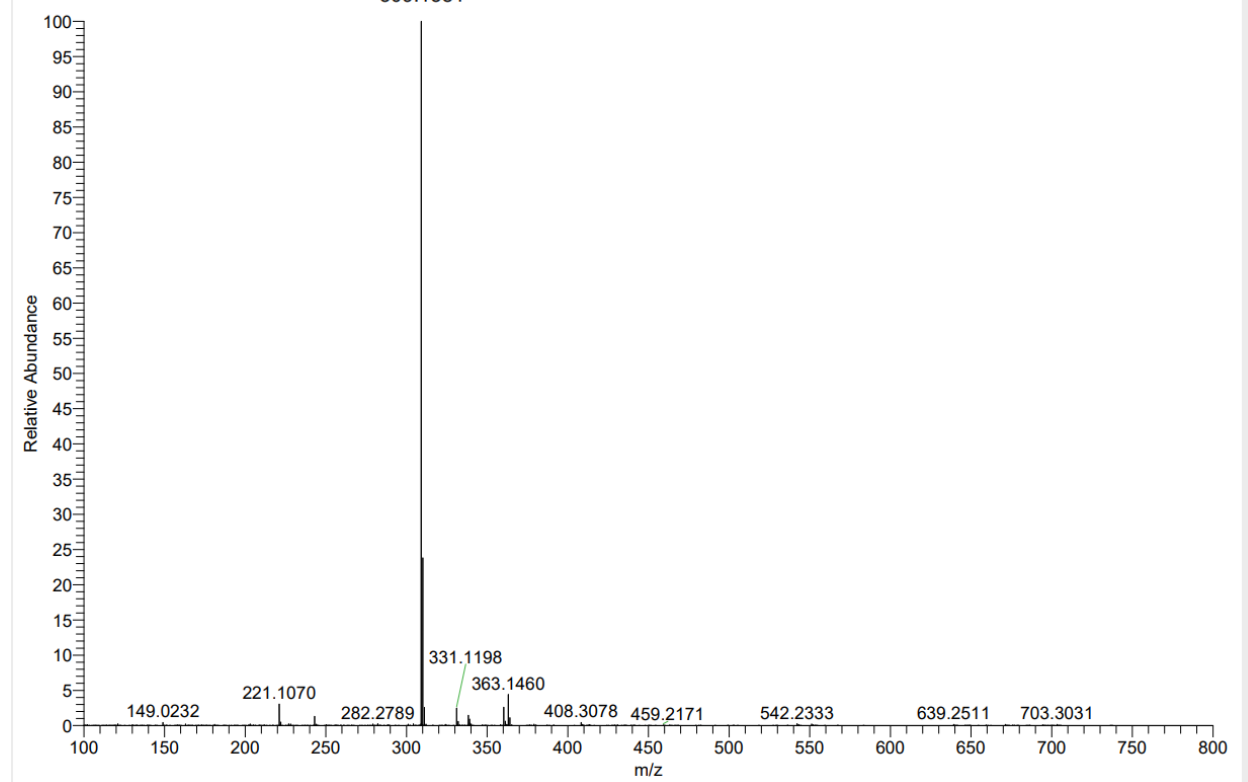
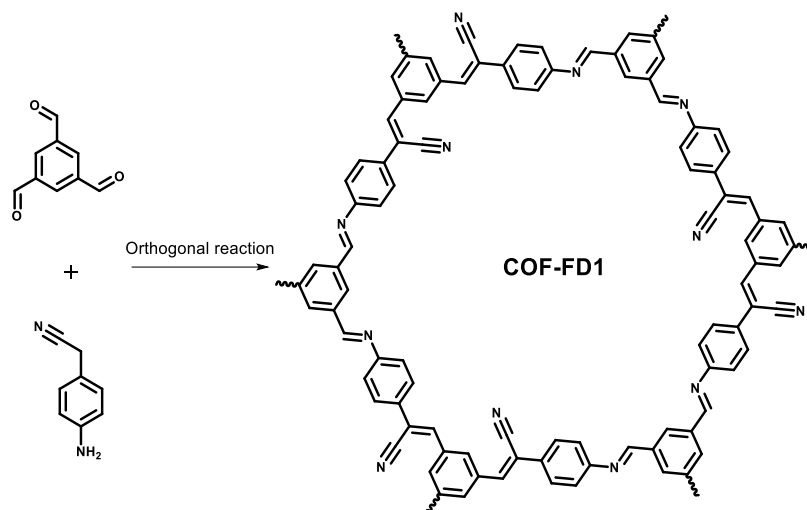


Figure S3. HRMS of BAPP.

Synthesis of COF-FD1



A 50 mL Schlenk tube was charged with 4-aminobenzyl cyanide (19.8 mg, 0.15 mmol) and TFB (16.2 mg, 0.1 mmol) in methanol (3 mL). Afterward, 0.4 mL of NaOH (4 M) was added to the mixture, and then the mixture was sonicated for 5 min and allowed to stand at room temperature for 2 days. Then, 0.6 mL of acetic acid (6 M) was added, and the mixture was further decompression degassed through the vacuum pump for 3 min. The tube was placed in an oil bath at 120 °C without disturbance for 2 days and then cooled to room temperature, and the precipitate was collected by filtration and sequentially washed twice with methanol, H₂O, DCM and DMF. This was followed by Soxhlet extraction in THF for 24 h and drying under vacuum at 105 °C for 12 h to afford a yellow powder (25 mg, 81%).

Section S3. Extensive screening of synthetic conditions

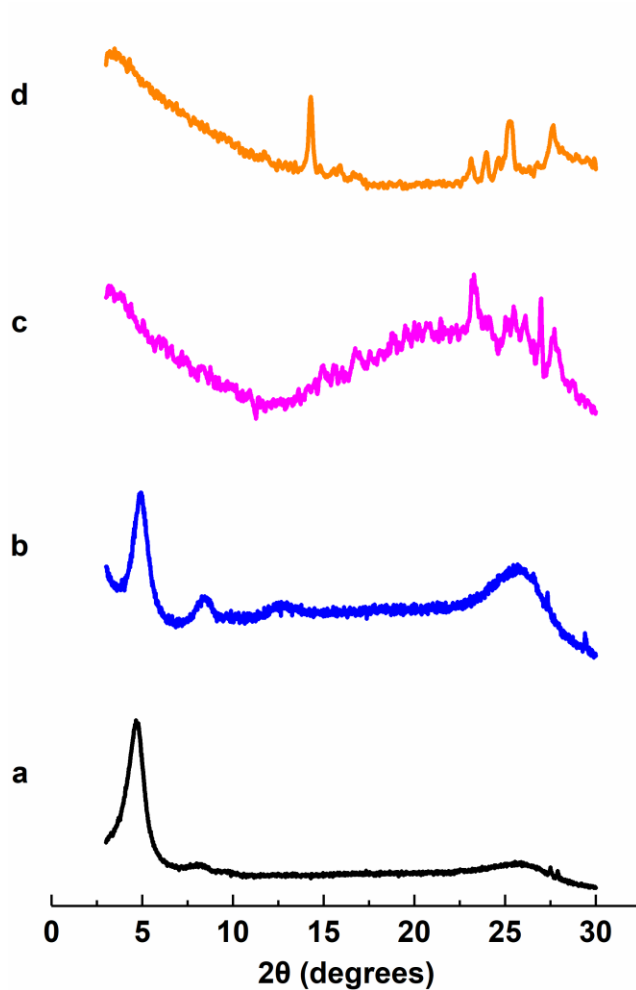


Figure S4. PXRD patterns of COF-FD1 synthesized in different solvents. a) methanol: *o*-dichlorobenzene = 1.5 mL: 1.5 mL; b) methanol: mesitylene = 1.5 mL: 1.5 mL; c) 1,4-dioxane: mesitylene = 1.5 mL: 1.5 mL; d) *n*-butanol: *o*-dichlorobenzene = 1.5 mL: 1.5 mL.

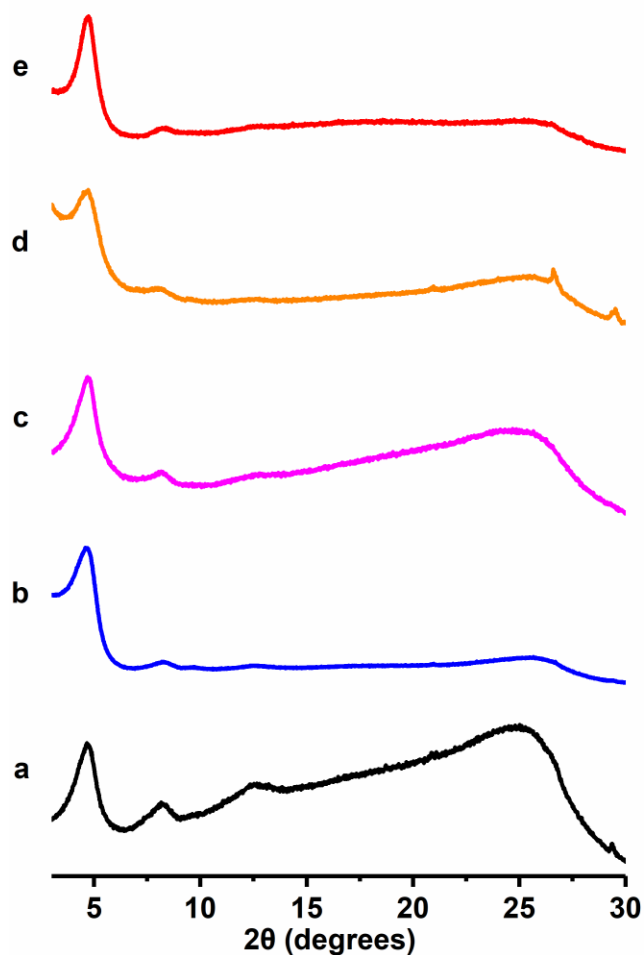


Figure S5. PXRD patterns of COF-FD1 synthesized with indicated conditions. a) methanol: 1,4-dioxane = 1.5 mL: 1.5 mL; b) methanol: mesitylene = 1.5 mL: 1.5 mL; c) methanol: 1-Methyl-2-pyrrolidinone = 1.5 mL: 1.5 mL; d) methanol: 1,2,4-trichlorobenzene = 1.5 mL: 1.5 mL; e) methanol: *o*-dichlorobenzene = 1.5 mL: 1.5 mL.

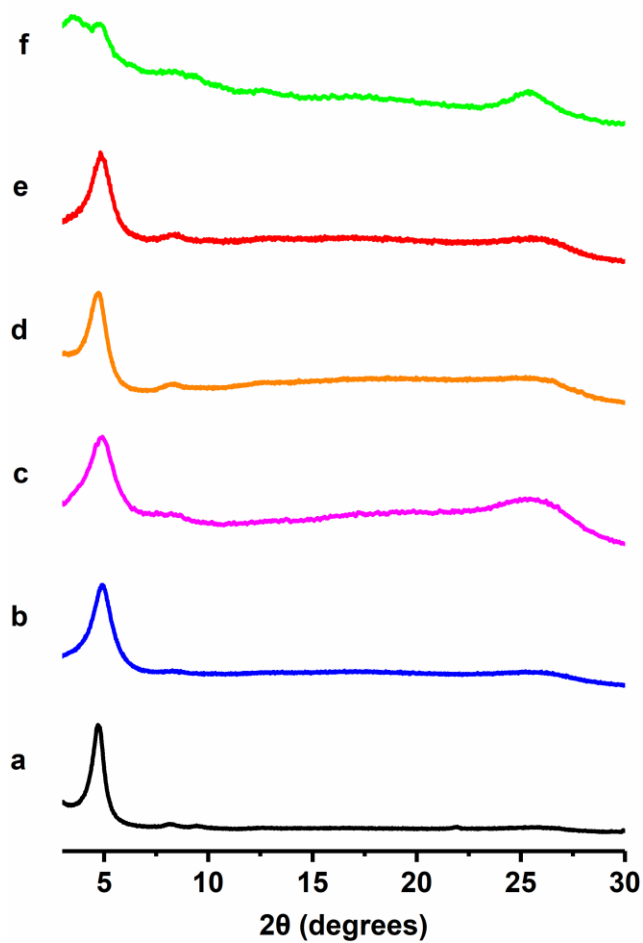


Figure S6. PXRD patterns of COF-FD1 synthesized with indicated conditions. a) methanol: *o*-dichlorobenzene = 3mL: 0 mL; b) methanol: *o*-dichlorobenzene = 2.5 mL: 0.5 mL; c) methanol: *o*-dichlorobenzene = 2 mL: 1 mL; d) methanol: *o*-dichlorobenzene = 1.5 mL: 1.5 mL; e) methanol: *o*-dichlorobenzene = 1 mL: 2 mL; f) methanol: *o*-dichlorobenzene = 0.5 mL: 2.5 mL.

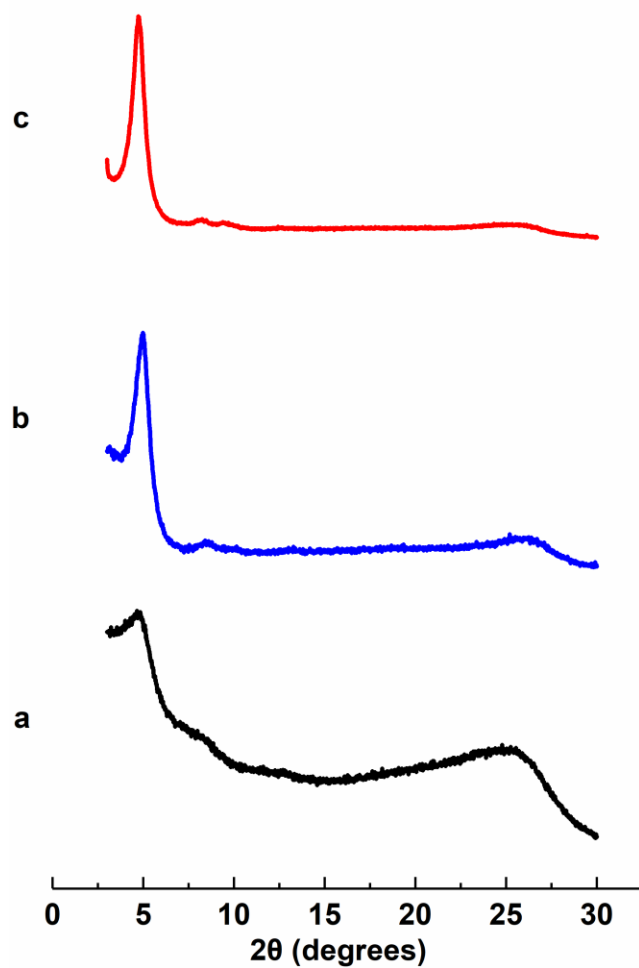


Figure S7. PXRD patterns of COF-FD1 synthesized with different concentrations of acetic acid in methanol solution. a) 3 M acetic acid; b) 4 M acetic acid; c) 6 M acetic acid.

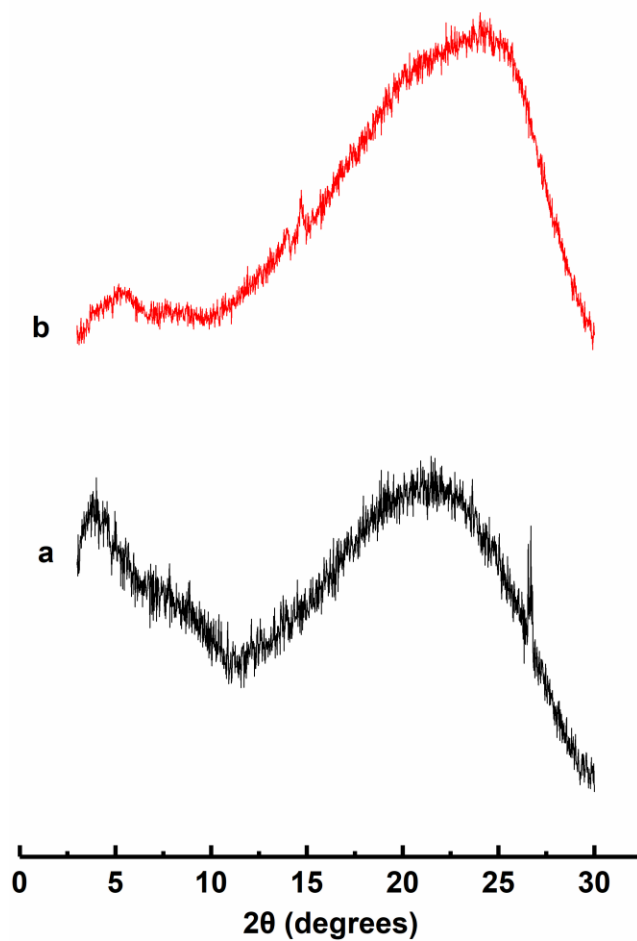


Figure S8. PXRD patterns of COF-FD1 synthesized without adding acetic acid in methanol solution. a) room temperature for 4 days; b) room temperature for 2 days, and then 120 °C heating for 2 days.

Section S4. FT-IR Spectra

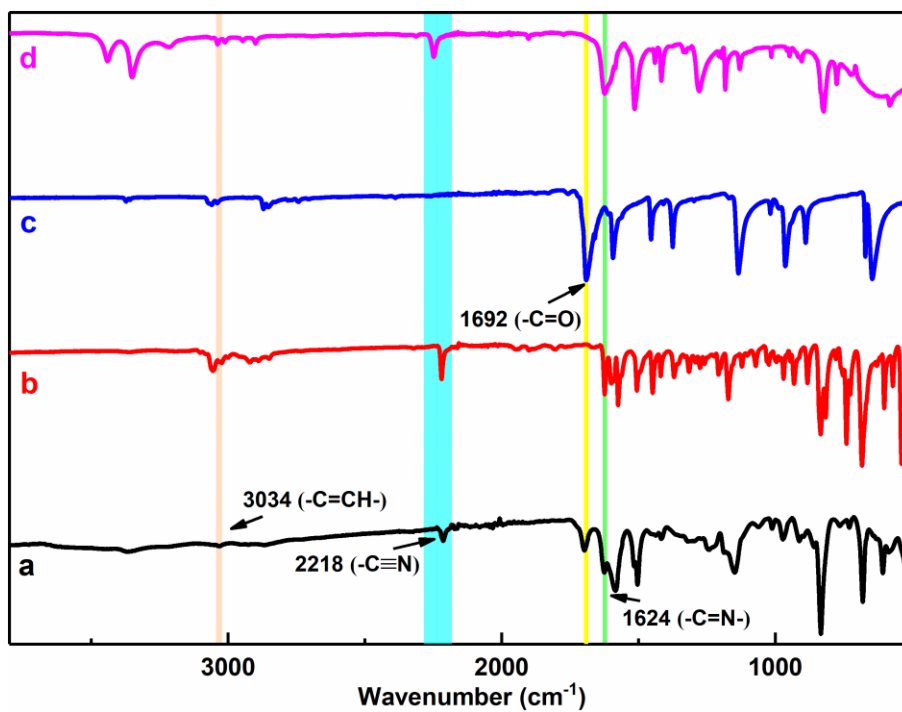


Figure S9. FT-IR spectra. a) COF-FD1 (black); b) model compound (BAPP) (red); c) TFB (blue); d) 4-aminobenzyl cyanide (purple).

Section S5. ^{13}C CP/MAS NMR Spectra

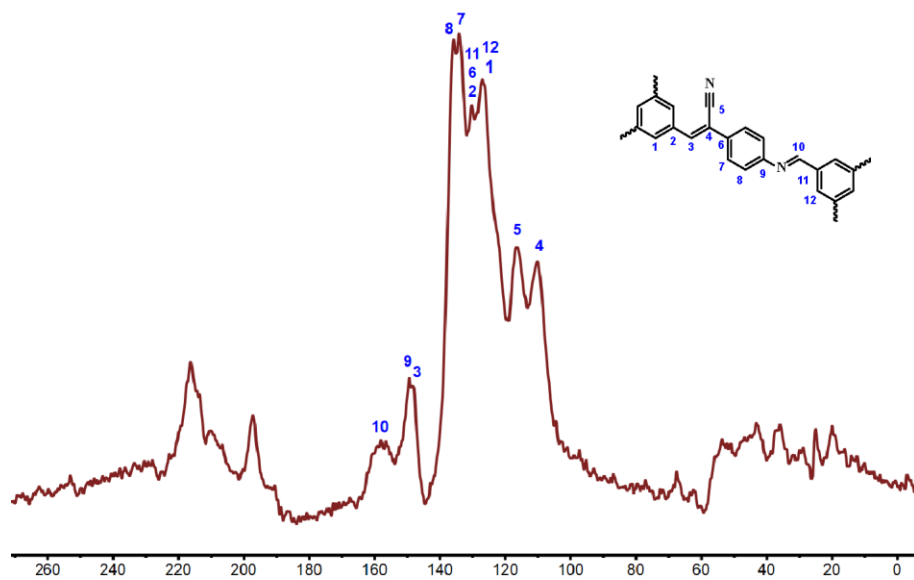


Figure S10. ^{13}C CP/MAS NMR spectrum of COF-FD1. The assignments of ^{13}C chemical shifts were figured out in the chemical structure.

Section S6. Structural Modeling Method and Powder X-Ray Diffraction Analysis

Structural Modeling Method

Molecular modeling of the COF-FD1 was generated using the Materials Studio (MS) software package. The initial lattice was created by starting with the space group $P3$, with the parameters of $a = b = 22.8572 \text{ \AA}$ and $c = 3.5 \text{ \AA}$. Firstly, we degraded the symmetry of lattice to $P1$, inserted a repeating module composed of monomers in the empty cell, omitted the redundant carbon atoms and all the hydrogen atoms, and promoted the symmetry to $P3$, outputting the crude structure of COF-FD1. Then the lattice model was geometry optimized using the MS Forcite molecular dynamics module (Universal Forcefields, Use current of Charges, Ewald summations). Subsequently, found symmetries and imposed symmetry to $P-6$, and automatically added hydrogen atoms, the lattice model was geometry optimized again using the MS Forcite molecular dynamics module (Universal Forcefields, using QEq of Charges, Ewald summations). Finally, Pawley refinement was applied to define the lattice parameters, producing the refined PXRD profile with lattice parameters of $a = b = 21.6031 \text{ \AA}$ and $c = 3.1222 \text{ \AA}$. R_{wp} and R_p values converged to 3.29% and 2.54% (Table S1 and Figure S11), respectively (Line broadening from the crystallite size and lattice strain were both concerned). Overlay of the observed and refined profiles shows good agreement (Figures S11 and S12). A staggered arrangement for COF-FD1 was also examined and the PXRD pattern calculated from this structure does not match the observed pattern (Figure S13), possibly ruling out this arrangement¹.

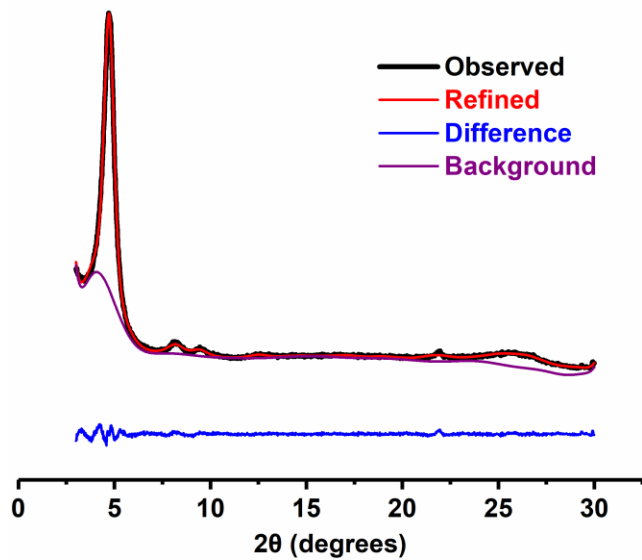


Figure S11. Pawley refinement of COF-FD1 with an eclipsed structure.

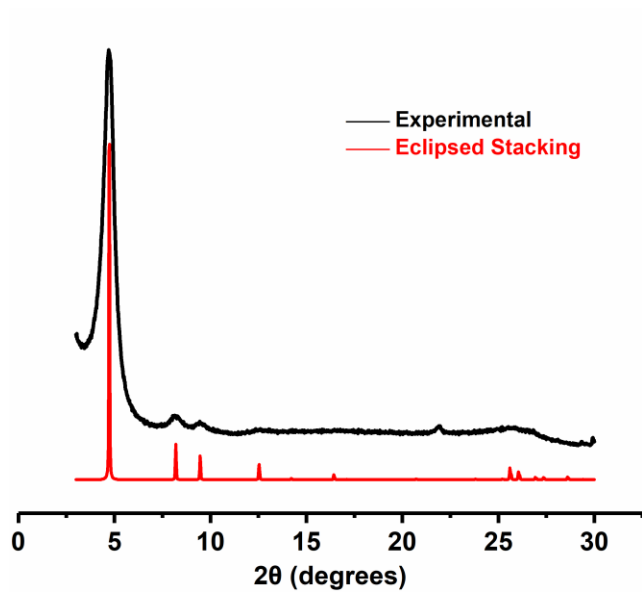


Figure S12. PXRD Pattern of COF-FD1 with an eclipsed stacking.

Table S1. Fractional atomic coordinates for the unit cell of COF-FD1 calculated from the Materials Studio modeling program after Pawley refinement.

COF-FD1: Space group symmetry <i>P-6 174</i>			
$a = b = 21.6031 \text{ \AA}$ $c = 3.1222 \text{ \AA}$			
$\alpha = \beta = 90^\circ$, $\gamma = 120^\circ$			
Atomic name	X(Å)	Y(Å)	Z(Å)
C1	1.07121	0.03879	-1
C2	1.03173	0.06966	-1
C3	1.14682	0.07481	-1
C4	1.19312	0.14146	-1
C5	1.26795	0.1669	-1
C6	1.29546	0.12389	-1
C7	1.36484	0.14978	-1
C8	1.40926	0.21867	-1
C9	1.38322	0.26225	-1
C10	1.31391	0.23679	-1
N11	1.47987	0.2414	-1
C12	1.52903	0.30307	-1
C13	1.17325	0.19184	-1
C14	1.15865	0.23322	-1
C15	1.59933	0.31805	-1
N16	1.61503	0.26645	-1
H17	1.05417	0.12287	-1
H18	1.1654	0.04043	-1
H19	1.26529	0.0701	-1
H20	1.38463	0.11593	-1
H21	1.41549	0.31593	-1
H22	1.29683	0.27285	-1
H23	1.51989	0.3447	-1
H24	1.57501	0.21466	-1

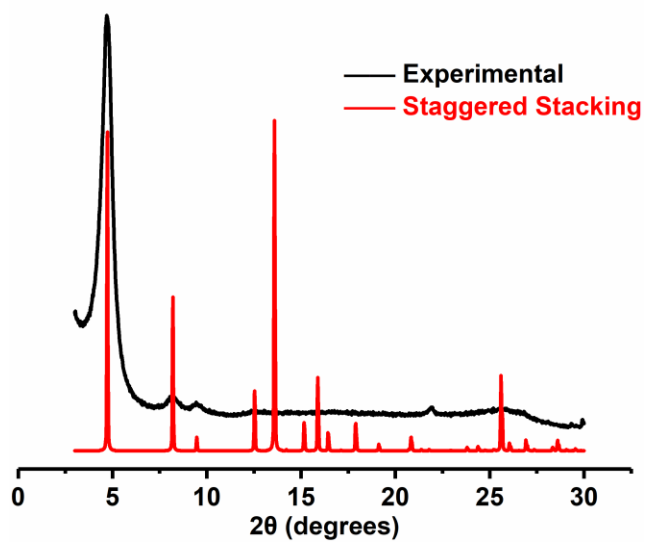


Figure S13. PXRD Pattern of COF-FD1 with a staggered stacking.

Section S7. Scanning Electron Micrographs Analysis

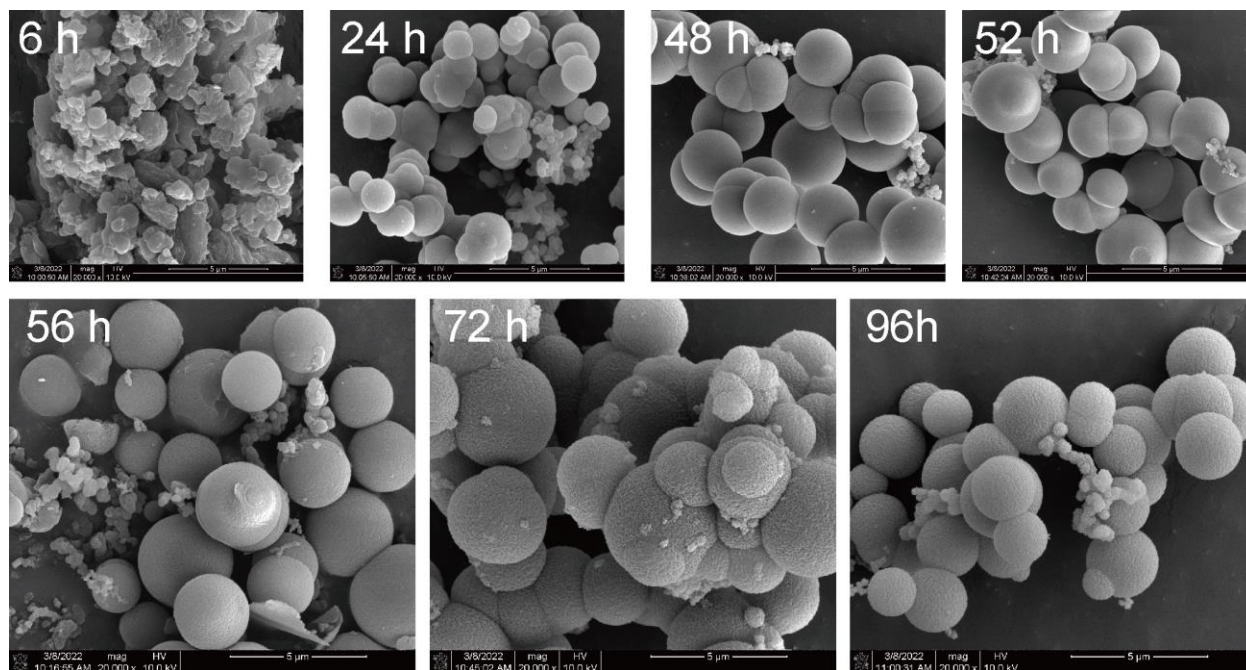


Figure S14. SEM images of COF-FD1 with spherical structure at different times.

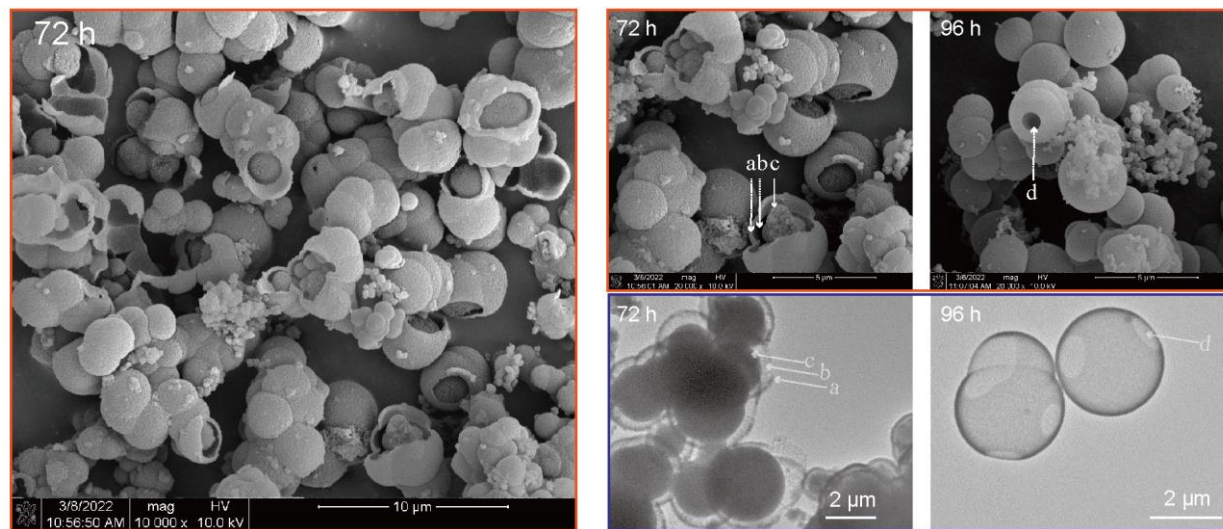


Figure S15. SEM (red frame) and TEM (blue frame) images of COF-FD1 with fractured spherical structure at 72 h and 96 h. a) shell; b) core-shell cavity space; c) inner core; d) complete cavity space.

Section S8. Transmission Electron Micrographs Section Analysis

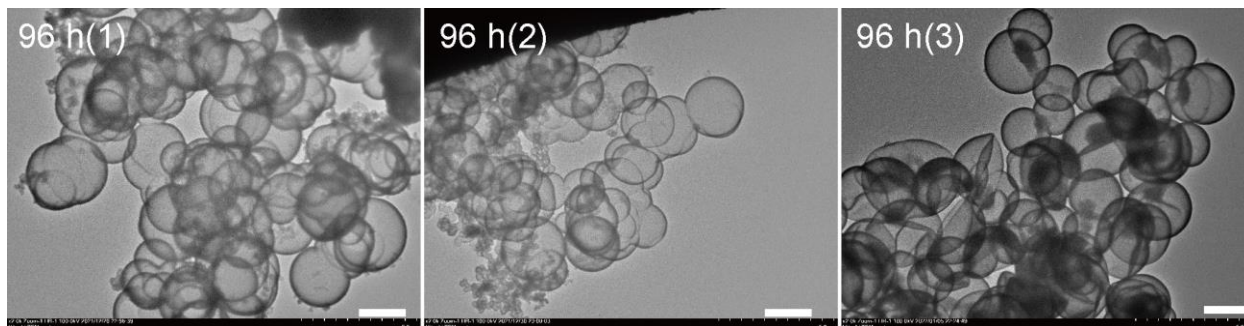


Figure S16. TEM images, 96 h (1), 96 h (2) and 96 h (3) represent COF-FD1 synthesized from different experimental batches. Scale Bar: 2 μm .

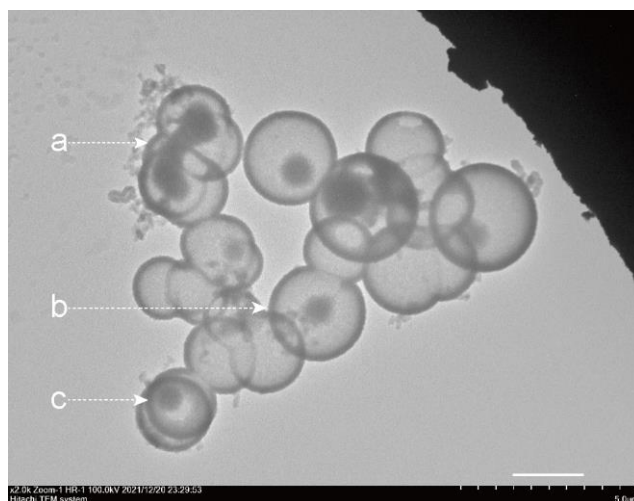


Figure S17. TEM images of COF-FD1 with three morphologies were observed simultaneously at 72 h. a) interconnected core-shell hollow spheres; b) symmetric core-shell hollow spheres; c) asymmetric core-shell hollow spheres. Scale Bar: 2 μm .

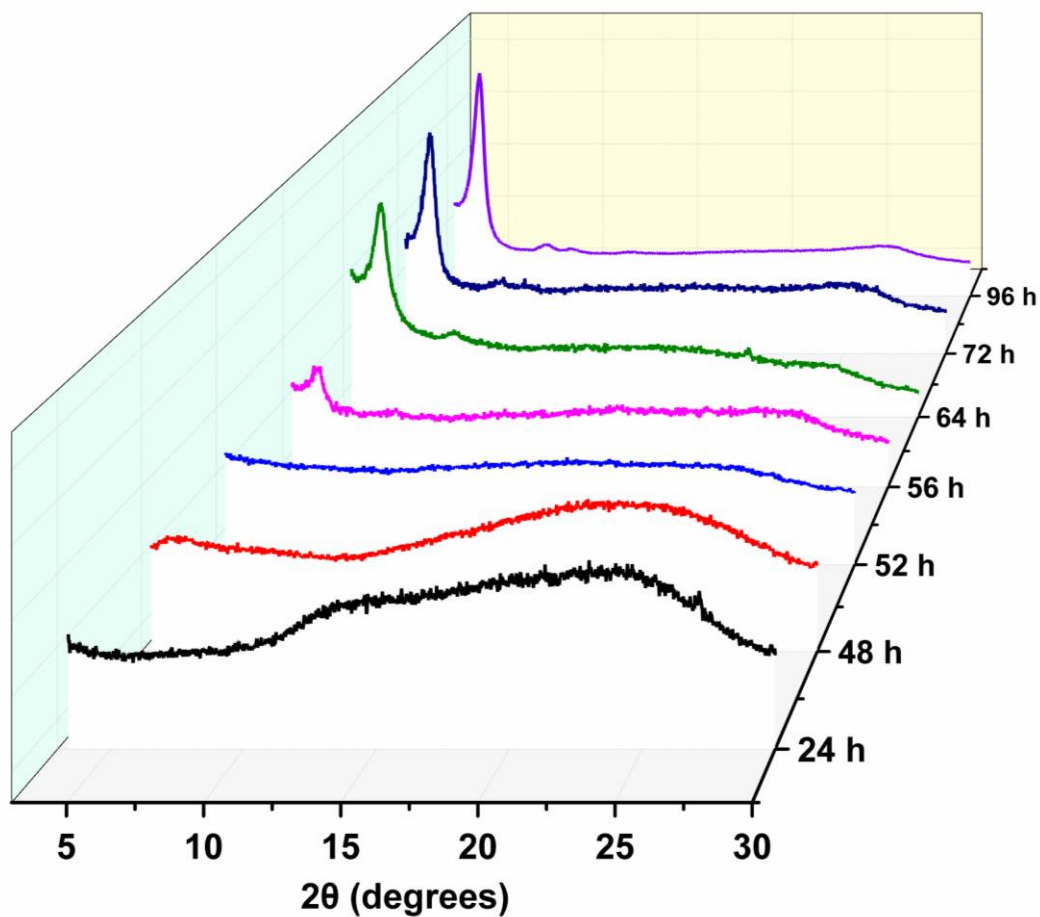


Figure S18. PXRD patterns of COF-FD1 prepared with different times.

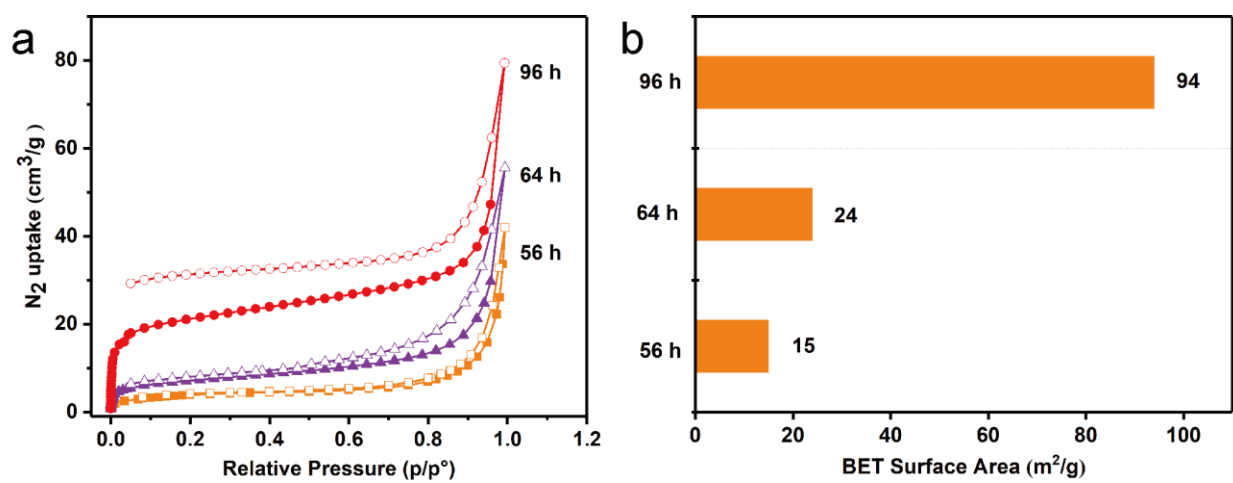


Figure S19. N_2 adsorption-desorption isotherms of COF-FD1 with different times.

Section S9. Thermogravimetric Analysis

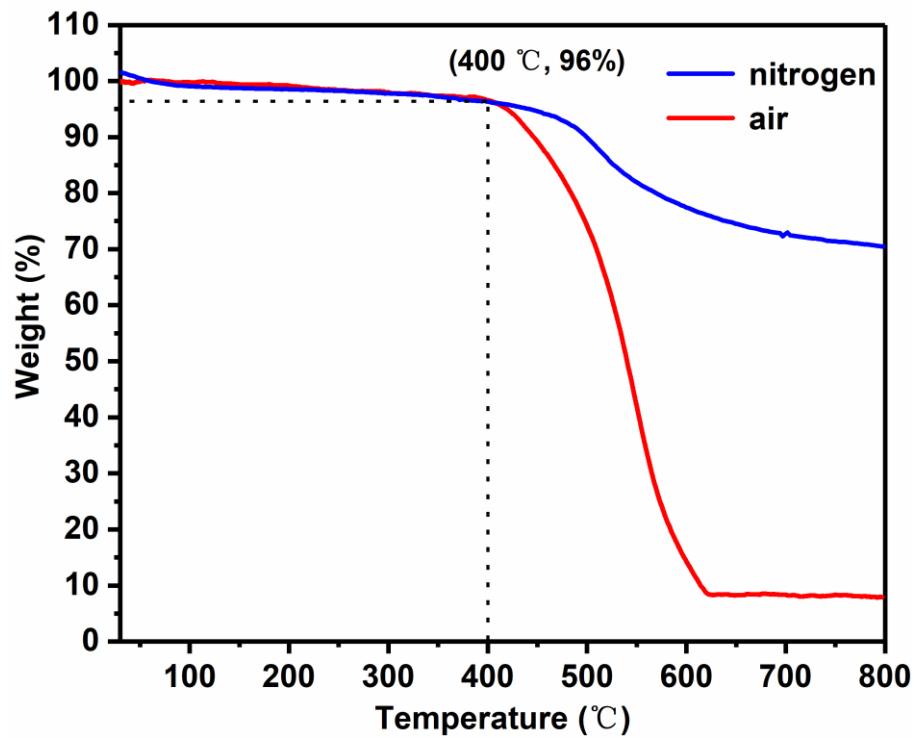


Figure S20. TGA data of COF-FD1 in different gas atmospheres.

Section S10. Chemical Stability Analysis

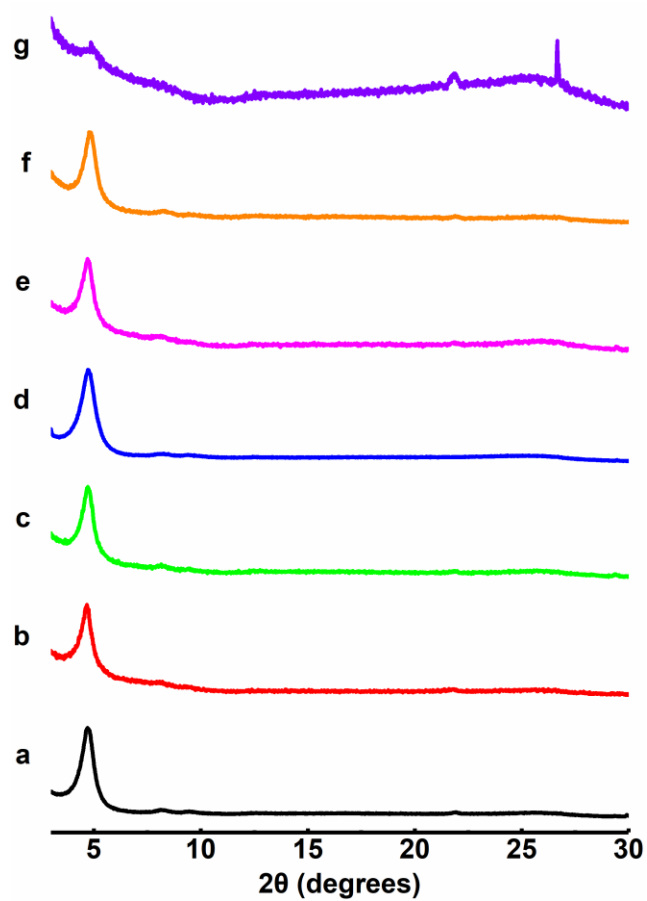


Figure S21. PXR D patterns of COF-FD1 after treatment with different solvents for 3 days. a) pristine; b) THF; c) H₂O; d) DCM; e) DMF; f) 4 M NaOH; g) 4 M HCl.

Section S11. Water contact angle on the surface of COF-FD1

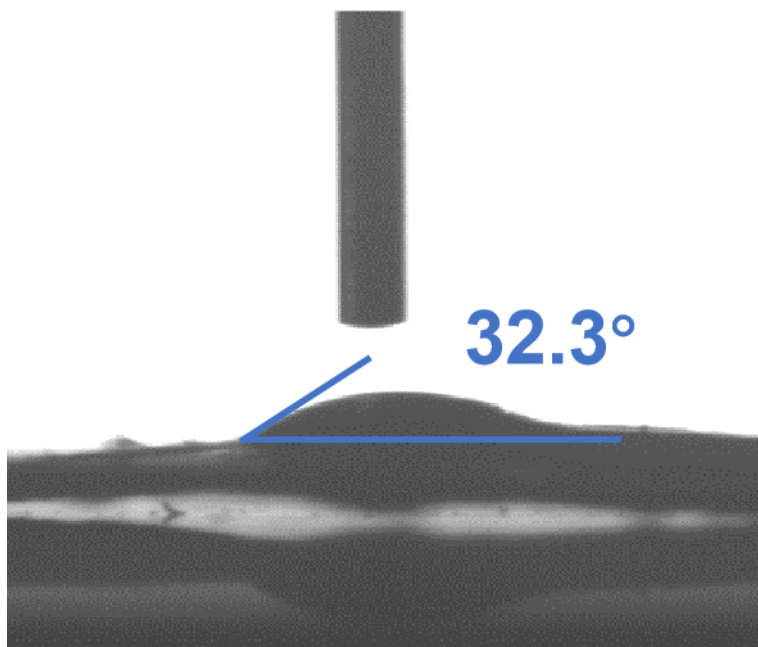


Figure S22. Water contact angle on the surface of COF-FD1.

Section S12. N₂ adsorption and desorption Analysis

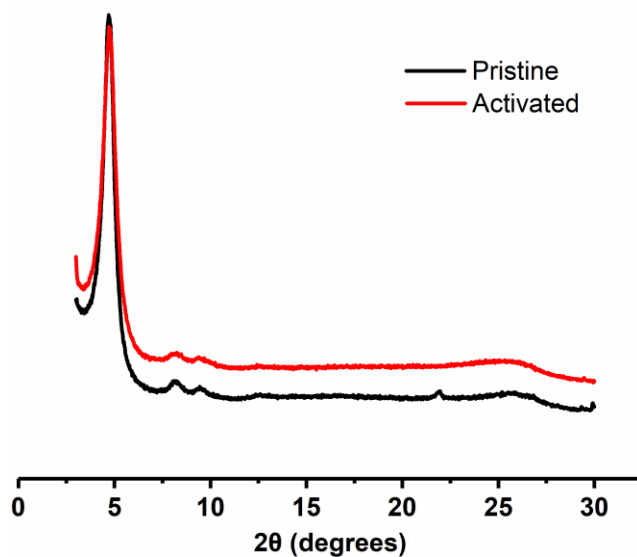


Figure S23. PXRD patterns of COF-FD1 after activated by vacuum at 105 °C for 12 h.

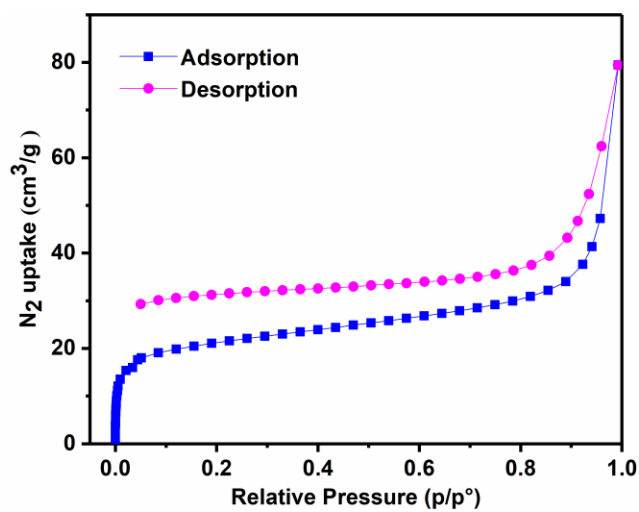


Figure S24. N₂ adsorption and desorption isotherms of COF-FD1 (96 h).

Section S13. Pore size distribution of COF-FD1

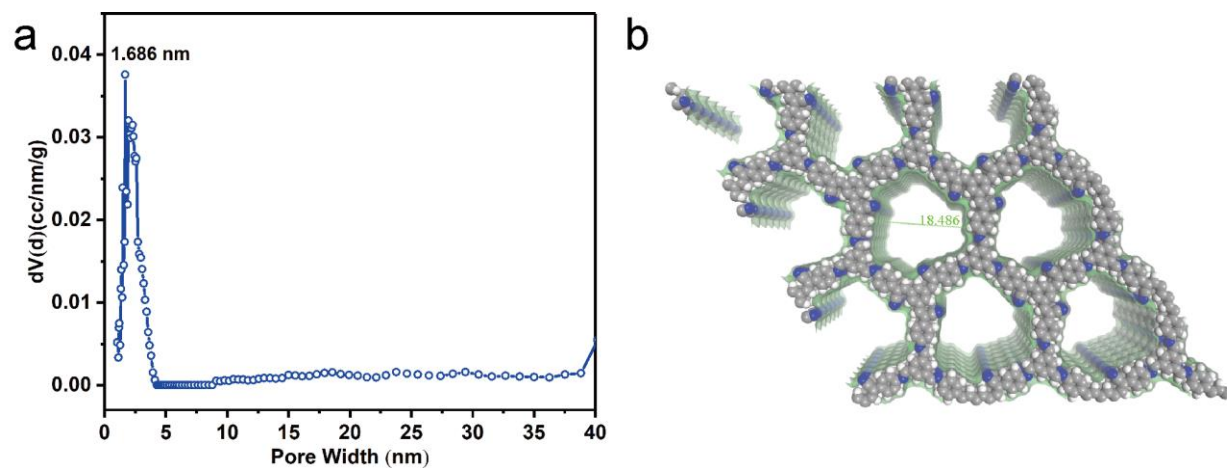


Figure S25. a) Pore size distribution of COF-FD1 estimated by NLDFT; b) Pore size of COF-FD1 simulated by Materials Studio.

Section S14. Fluorescence spectra

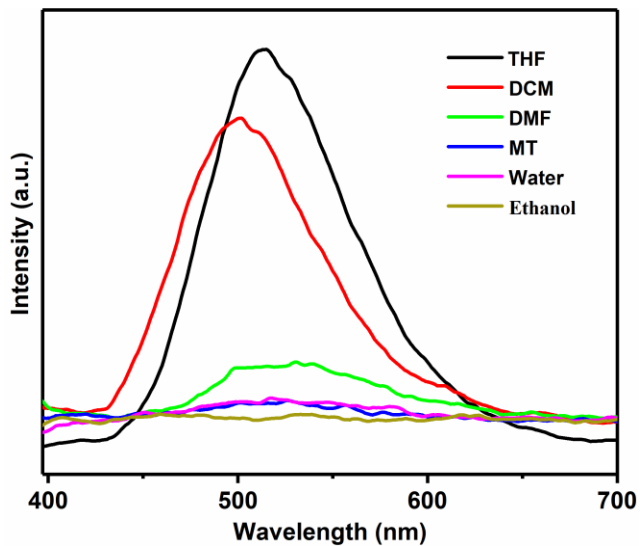


Figure S26. Fluorescence spectra of COF-FD1 in different common solvents.

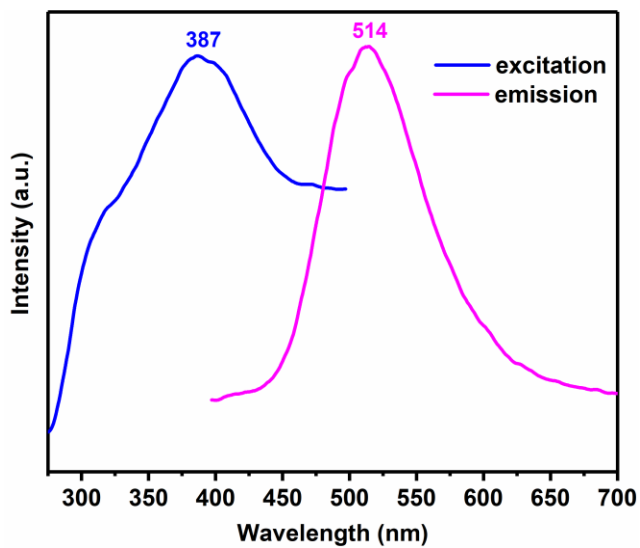


Figure S27. The fluorescence excitation (blue) and emission (pink) spectra of COF-FD1.

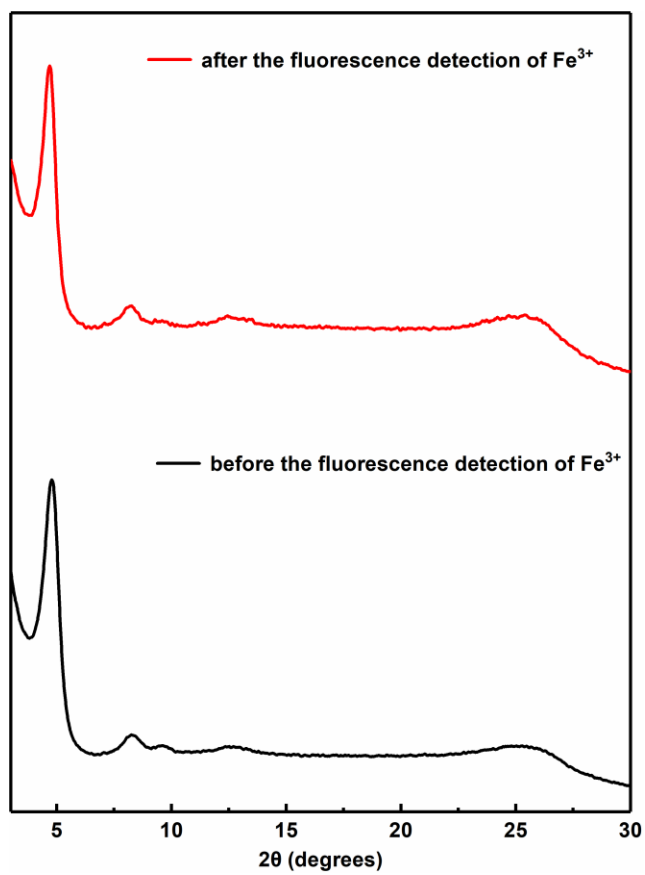


Figure S28. PXRD patterns of COF-FD1 before and after the fluorescence detection of Fe^{3+} .

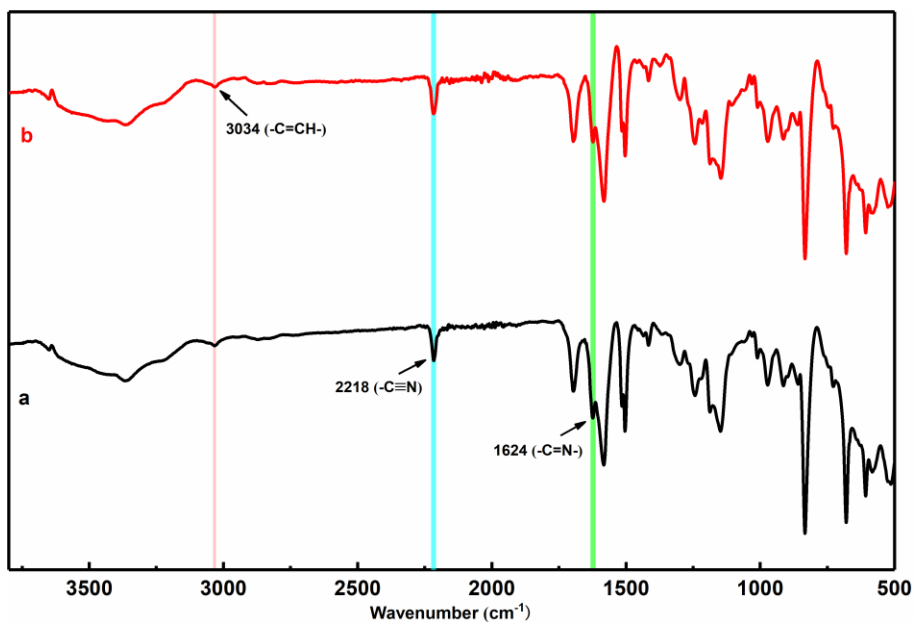


Figure S29. FT-IR spectra. a) before the fluorescence detection of Fe³⁺; b) after the fluorescence detection of Fe³⁺.

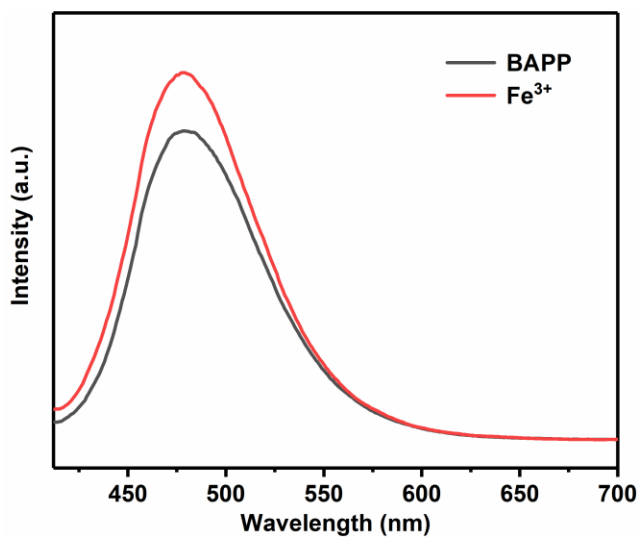


Figure S30. Fluorescence emission spectra of model compound (BAPP) (0.1mg/10 mL) before and after addition of Fe³⁺ ions in THF solution (E_x:402 nm, E_m:478 nm).

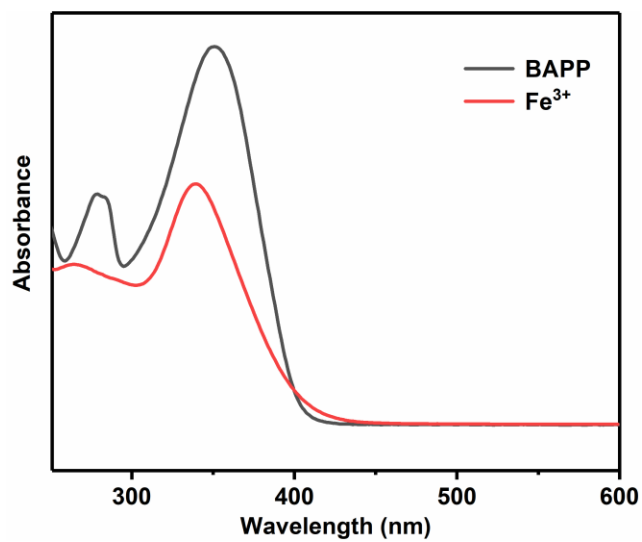


Figure S31. The UV-Vis absorption spectra of Fe³⁺ ions and BAPP in THF solution.

Section S15. References

(1) Ding, S. Y.; Gao, J.; Wang, Q.; Zhang, Y.; Song, W. G.; Su, C. Y.; Wang, W. Construction of Covalent Organic Framework for Catalysis: Pd/COF-LZU1 in Suzuki-Miyaura Coupling Reaction. *J. Am. Chem. Soc.* 2011, *133*, 19816-19822.